Zeng *et al. Chem Synth* 2022;2:12
DOI: 10.20517/cs.2022.11

Chemical Synthesis

Short Communication

Open Access

Coordination-driven [2+2] metallo-macrocycles isomers: conformational control and photophysical properties

Yunting Zeng[1], Junjuan Shi[1], Kehuan Li[1], Jiaqi Li[1], Hao Yu[1], Fang Fang[2], Xin-Qi Hao[3], Houyu Zhang[1], Ming Wang[1,*]

[1]State Key Laboratory of Supramolecular Structure and Materials, College of Chemistry, Jilin University, Changchun 130012, Jilin, China.
[2]Instrumental Analysis Center, Shenzhen University, Shenzhen 518055, Guangdong, China.
[3]College of Chemistry and Green Catalysis Center, Zhengzhou University, Zhengzhou 450001, Henan, China.

Correspondence to: Prof. Ming Wang, State Key Laboratory of Supramolecular Structure and Materials, College of Chemistry, Jilin University, No. 2699 Qianjin Street, Changchun 130012, Jilin, China. E-mail: mingwang358@jlu.edu.cn

How to cite this article: Zeng Y, Shi J, Li K, Li J, Yu H, Fang F, Hao XQ, Zhang H, Wang M. Coordination-driven [2+2] metallo-macrocycles isomers: conformational control and photophysical properties. *Chem Synth* 2022;2:12. https://dx.doi.org/10.20517/cs.2022.11

Received: 12 May 2022 **First decision:** 8 Jun 2022 **Revised:** 14 Jun 2022 **Accepted:** 27 Jun 2022 **Published:** 30 Jun 2022

Academic Editors: Bao-Lian Su, Teng Ben **Copy Editor:** Jia-Xin Zhang **Production Editor:** Jia-Xin Zhang

Abstract

In recent years, fluorescent supramolecular materials have received significant attention due to their wide application prospects. However, the relationship between the conformation of supramolecules and their photophysical properties remains an open question. In this study, two rhomboidal metallacycle isomers, **SA** and **SB,** self-assembled with trans- and cis-isomers of tetraphenylethylene-based ditopic pyridyl ligands (**LA** and **LB**), and a 120° di-platinum (II) acceptor were prepared. Compared with metallacycle **SB** constructed by cis-tetraphenylethylene (TPE)-based ligand **LB**, the curved rhomboidal metallacycle **SA** constructed with trans-TPE-based ligand **LA** can restrict molecular motions of the aromatic groups on TPE and exhibits better light-emitting properties. Moreover, curved **SA** also exhibited better fluorescence stability than isomer **SB** towards molecules with strongly electron-withdrawing groups. This work provides a new platform to explore the relationship between conformation and the corresponding photophysical properties.

Keywords: Supramolecular self-assembly, metallacycles, isomer, conformational control, coordination-induced emission

INTRODUCTION

In the past decades, fluorescence materials have attracted considerable attention for their widespread applications in biological imaging[1], environmental sensing[2], fluorescent probes[3], and other fields[4] due to their high luminous efficiency and stimulus responsiveness. However, conventional organic fluorophores often suffer from aggregation-caused quenching (ACQ) in a concentrated solution or the solid state, which limits their practical application[5]. To overcome the undesirable ACQ, in 2001, Tang and co-workers developed fluorescent species exhibiting the opposite effect, known as aggregation-induced emission (AIE)[6]: tetraphenylethylene (TPE), 1,1,2,3,4,5-hexaphenylsilole, triphenylamine, distyrylanthracene, etc[7]. The characteristic of molecules with AIE activity is that their initial free rotation is restricted in an aggregation state, resulting in reduced non-radiative decay and strong fluorescence emission. However, AIE active molecules have relatively low luminous efficiency in dilute solution because the free rotation of benzene rings leads to high non-radiative decay.

Among the diverse field of supramolecular chemistry, coordination-driven self-assembly offers a straightforward synthetic approach for constructing diverse metal-organic complexes (MOCs)[8], ranging from two-dimensional (2D) metallacycles to three-dimensional (3D) metallacages. The metal coordination bonds not only provide definite directionality and high predictability but also have moderate bond energies (15-25 kcal/mol) to ensure self-modulation and thermodynamic stability during self-assembly. These unique advantages allow MOCs to be well constructed with specific stoichiometry and precise geometry and, thus, provide the impetus for applications in catalysis, sensing, and optics[9]. Recently, MOCs combined with AIEgens have also drawn particular attention as multifunctional platforms for exploring AIE properties. However, how to provide the bright emission of AIEgens in dilute solution is still a big challenge. Rational synthesis strategies should be developed to restrict the rotation of phenyl rings by slightly adjusting the conformation of the AIE group via metal coordination. In this way, the non-radiative decay in the excited state can be further reduced, thus giving a bright emission in dilute solution, which is also known as coordination-induced emission (CIE).

Herein, we provide such a CIE strategy via constructing two rhomboidal metallacycle isomers **SA** and **SB** by the self-assembly of trans- and cis-isomers of TPE-based ditopic pyridyl ligands (**LA** and **LB**) with a di-platinum (II) acceptor. It is worth mentioning that these two ligands can be easily obtained through one-pot synthesis and separation by column chromatography. In contrast to **SB** constructed by cis-TPE-based ligand **LB**, the curved rhomboidal metallacycle **SA** based on trans-TPE-based ligand **LA** could restrict molecular motions of the TPE aromatic groups, inducing the integration of AIE and CIE and thus showing double the quantum yield as **SB**. Moreover, curved **SA** also exhibited better fluorescence stability than isomer **SB** towards strongly electron-withdrawing molecules.

RESULTS AND DISCUSSION

The synthesis and characterization of the 120° di-Pt(II) acceptor **1** and the two ditopic ligands **LA** and **LB** are shown in the supplementary materials [Supplementary Figures 1-11]. The two isomeric ligands **LA** and **LB** can be obtained in a 1:1 product ratio by one-pot Suzuki coupling reactions and column chromatography (SiO_2). As shown in Scheme 1, the obtained 180° trans-TPE-based ligand **LA** and 60° cis-TPE-based ligand **LB** were assembled with the same 120° di-Pt(II) acceptor **1** in a 1:1 stoichiometric ratio in DMSO at 80 °C, affording the metallacycles **SA** and **SB**, respectively. After 10 h, the final discrete metallacycles were obtained in quantitative yields (94% for **SA** and 92% for **SB**) by sedimentation and centrifugation.

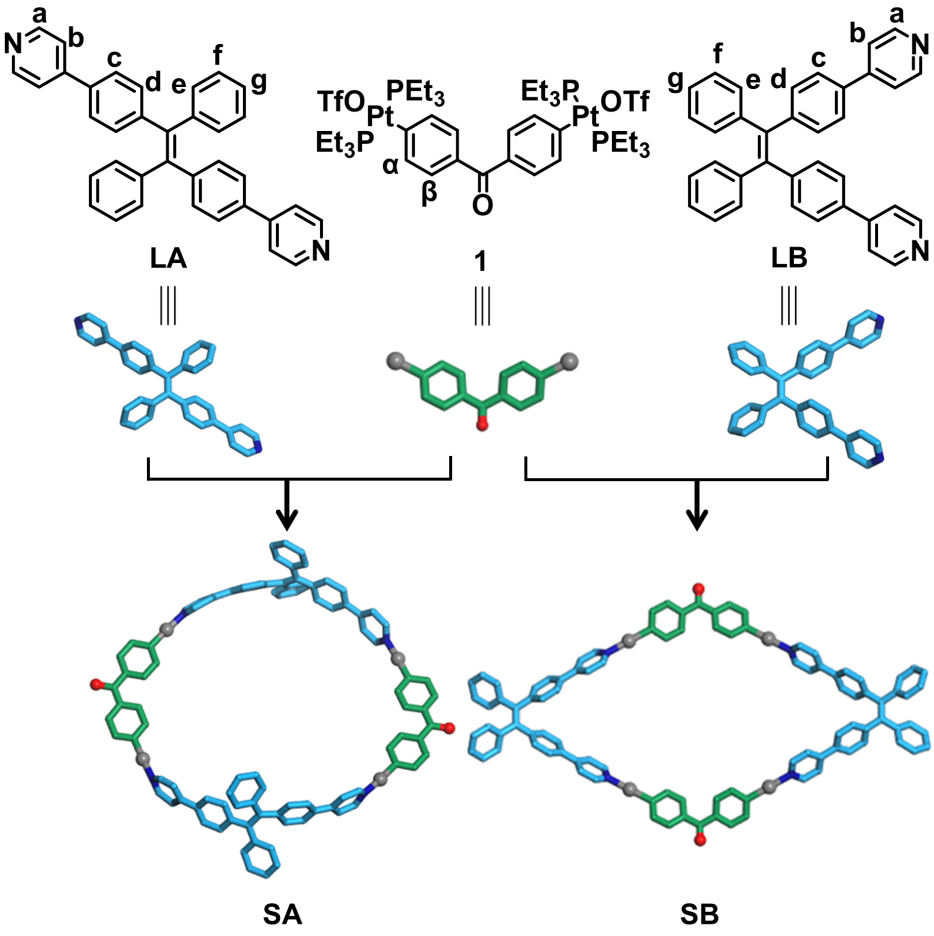

Scheme 1. Self-assembly of metallacycles **SA** and **SB** (energy-minimized structures). Carbon atoms of ligands **LA** and **LB** are blue, carbon atoms of acceptor **1** are green, nitrogen atoms are dark blue, oxygen atoms are red, phosphorus atoms are pink, and platinum atoms are grey.

The formation of discrete metallacycles **SA** and **SB** with highly symmetric architecture was first investigated by multinuclear NMR analysis [^{1}H, ^{31}P{^{1}H}, ^{13}C, 2D correlation spectroscopy, and 2D diffusion-ordered NMR spectroscopy (DOSY)] [Figure 1A-H and Supplementary Figures 12-23]. It is evident from the ^{1}H NMR spectra [Figure 1A-E] that no linear structures were formed. If a linear structure were formed, the proton signal of the ligands in these complexes would show more peaks due to the asymmetric chemical environment. In the ^{1}H NMR spectra [Figure 1A-E], the signals of protons corresponding to the pyridyl units and phenyl rings in metallacycles **SA** and **SB** exhibited downfield shifts relative to those of the free TPE ligands due to the loss of electron density after the formation of Pt-N coordination bonds. For metallacycle **SB**, the signals of the pyridyl and phenyl protons split into two sets upon metal coordination, being consistent with the previously reported MOC structures[10]. 2D diffusion-ordered spectroscopy (DOSY) in DMSO-d_6 showed a single band at log D = -10.19 for **SA** and -10.26 for **SB** [Supplementary Figures 17 and 23] further proving the formation of a single discrete structure. The diameters of **SA** and **SB** derived from the log D values by the Stokes-Einstein equation were 3.04 and 3.58 nm in DMSO, respectively, which matched well with the size of the expected structure. The ^{31}P{^{1}H} NMR spectrum of di-Pt(II) acceptor **1** and metallacycle **SA** both exhibited a single peak with concomitant ^{195}Pt satellites (δ = 18.99 ppm for **1** and δ = 13.16 ppm for **SA**) [Figure 1F and G]. However, the ^{31}P{^{1}H} NMR spectrum of metallacycle **SB** exhibited doublets (ca. 13.14 and 13.19 ppm) with concomitant ^{195}Pt satellites,

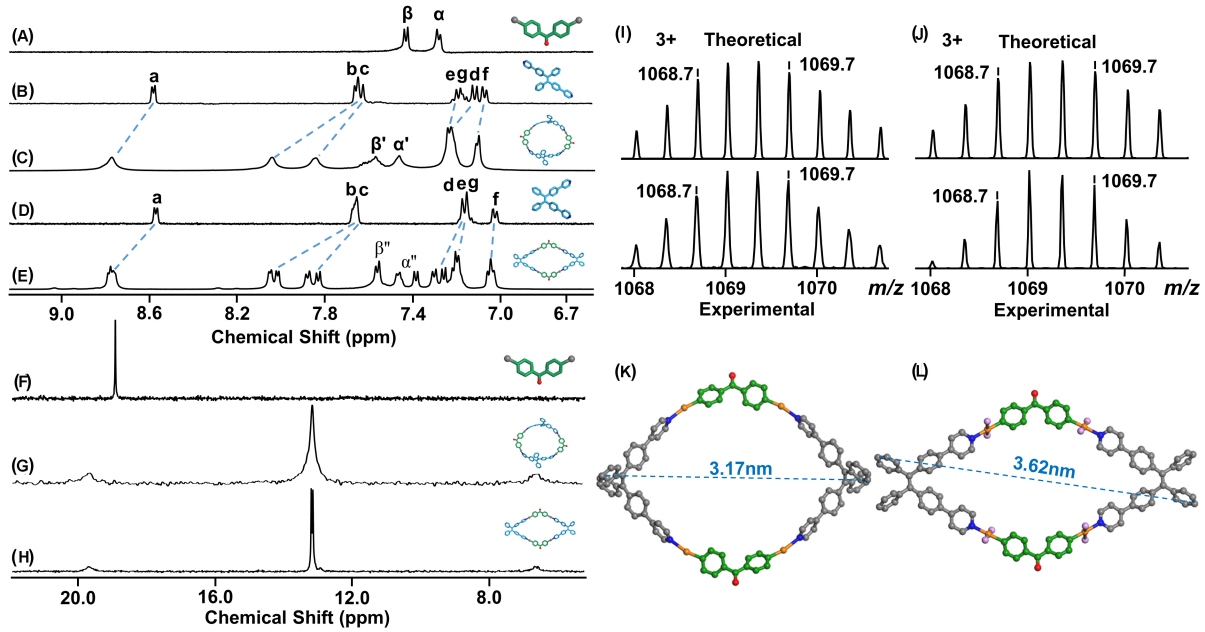

Figure 1. ^{1}H NMR spectra (500 MHz, 300 K) in DMSO-*d6* of: **1** (A); **LA** (B); **SA** (C), **LB** (D); and **SB** (E). ^{31}P{^{1}H} NMR spectra (500 MHz, 300 K) in DMSO-*d6* of: **1** (F); **SA** (G); and **SB** (H). ESI-MS spectra of **SA** (I) and **SB** (J). DFT-optimized ground-state structure of **SA** (K) and single-crystal X-ray structure of **SB** (L). Carbon atoms of ligands **LA** and **LB** are gray, carbon atoms of acceptor **1** are green, nitrogen atoms are dark blue, oxygen atoms are red, phosphorus atoms are pink, and platinum atoms are orange. Hydrogens and counterions OTf^- (trifluoromethanesulfonate) anions are omitted for clarity.

which could be attributed to the different chemical environments of phosphorus inside and outside the metallacycle [Figure 1H][11]. Compared with di-Pt(II) acceptor **1**, these peaks were shifted upfield by approximately 5.83 and 5.82 ppm for **SA** and **SB**, respectively. Furthermore, electrospray ionization mass spectrometry (ESI-MS) proved effective in determining the molecular formation of the obtained assemblies. One set of peaks with different charge states in the **SA** and **SB** systems was observed from the full ESI-MS spectra, due to the loss of different numbers of OTf^- counterions [Supplementary Figures 24 and 25]. In the ESI-MS spectrum of **SA** [Figure 1I and Supplementary Figure 26], a peak at m/z = 1068.7 Da corresponding to $[M\text{-}3OTf]^{3+}$ was observed. After the deconvolution of m/z, the molecular weight of **SA** was calculated to be 3652.94 Da, demonstrating the formation of a [2+2] assembly. Metallacycle **SB** showed the same fragments as obtained for **SA** (m/z = 1068.7 for $[M\text{-}3OTf]^{3+}$, m/z = 1677.5 for $[M\text{-}2OTf]^{2+}$ [Figure 1J and Supplementary Figure 27] and had the same molecular weight (for the relevant calculation method, see Section 4 of the Supplementary Materials). These peaks were isotopically resolved and in good agreement with their calculated theoretical distributions, indicating the formation of distinct metallacycle structures **SA** and **SB**. We failed to obtain single crystals of **SA** suitable for X-ray scattering due to its curved configuration that restricted the easy stacking of the metallacycle molecules. Instead, density functional theory (DFT) calculations were performed to simulate the supramolecular structures of **SA** [Figure 1K]. Fortunately, single crystals of **SB** were successfully obtained by slowly diffusing isopropyl ether into the acetone solution of **SB** over four weeks; the corresponding single-crystal structure is shown in Figure 1L. The detailed crystal information is shown in Supplementary Figures 28 and 29 and Supplementary Table 1. From the optimized structure of **SA** and the crystal structure of **SB**, it is evident that both were rhomboidal metallacycles, and **SA** exhibited a certain degree of bending. This unique structural feature laid a solid foundation for subsequent studies on the different luminous behaviors of the metallacycles.

After the successful construction of metallacycles **SA** and **SB**, their photophysical properties were studied. The absorption spectra of ligands and metallacycles are shown in Figure 2A. Ligands **LA** and **LB** displayed two similar broad absorption bands at 270 and 330 nm, originating mainly from pyridine and TPE. Due to the metal to ligand charge transfer (MLCT) after coordination and forming **SA** and **SB**, the two absorption bands were, respectively, red-shifted to 315 and 355 nm in SA and 315 and 365 nm in SB. Moreover, these assemblies exhibited significantly enhanced molar absorption coefficients because of the inclusion of two ligands in one metallacycle structure. Next, fluorescence spectra of ligands and metallacycles were also recorded [Figure 2B]. Ligands **LA** and **LB** showed weak emission at 485 nm in DMSO, which can be ascribed to the non-radiative relaxation pathway via intramolecular rotations of the phenyl and pyridyl rings. After assembling ligands into rhomboidal metallacycles, the emission intensity was enhanced and red-shifted by ~20 nm (505 nm). Compared to the normal rhombus metallacycle **SB**, the molecular motions of the aromatic groups on TPE are more restricted by coordination bonds in the curved metallacycle **SA**, decreasing the non-radiative decay and thus giving a brighter emission. Consequently, the obtained Φ_F value of **SA** in DMSO was 6.47%, significantly higher than the Φ_F of **SB** in DMSO (3.21%). The absorption and emission spectra of metallacycles **SA** and **SB** in the solid state were further explored [Supplementary Figure 30A]. Two similar broad absorption bands at 320 and 430 nm were observed from solid **SA** and **SB**. Solid **SA** also exhibited a long-wavelength absorption band centered at 525 nm, mainly corresponding to intramolecular charge transfer. Interestingly, a different fluorescence emission behavior was observed for metallacycles **SA** and **SB** in the solid state. Again, the intensity of the maximum emission peak of **SB** was significantly lower than that of **SA** and was 30 nm red-shifted compared with **SA.** Notably, the Φ_F values of metallacycles **SA** and **SB** in solid state were 26.17% and 23.14%, respectively, which were substantially higher than those obtained in the solution and displayed a typical AIE effect [Supplementary Figure 30B].

To investigate the AIE properties of metallacycles **SA** and **SB**, their fluorescence emission spectra in DMSO and DMSO/H_2O mixture solutions were recorded [Figure 2]. Adding water to the DMSO solution reduced the solubility of **SA** and **SB**, thereby promoting aggregate formation. Upon successive increments in the water content, the fluorescence intensities of **SA** chronologically increased and reached a maximum at 90% H_2O content [Figure 2C]. Its fluorescence quantum yield continued to increase with the rising water content and matched well with the change in fluorescence emission intensity [Figure 2D]. As anticipated, the fluorescence results demonstrate the AIE behavior of **SA**. Metallacycle **SB** displayed a similar AIE phenomenon [Figure 2E and F]. Interestingly, in the aggregated states (H_2O content = 90%), the fluorescence intensity of **SA** increased up to 27 times (Φ_F = 60.28%), whereas **SB** displayed only a 14-fold fluorescence enhancement (Φ_F = 26.08%). The more curved structure of metallacycle **SA** may promote the tight packing of TPE units in the aggregated state, enhancing its fluorescence remarkably. Moreover, the restricted movement of phenyl rings of TPE in **SA** further enriched its fluorescent performance compared to **SB**.

AIE-active molecules often show the phenomenon of fluorescence quenching due to the charge transfer between AIE moieties and molecules with strongly electron-withdrawing groups. Thus, we expected that the twisted and high luminous efficient structure of **SA** could effectively reduce the charge transfer process and quenching phenomenon. Inspired by the excellent AIE luminescence properties observed for rhombus metallacycles **SA** and **SB** in this study, we investigated the fluorescence stability of these two isomers in the DMSO/H_2O mixture with 90% H_2O content towards 2,4,6-trinitrotoluene (TNT). The quenching processes could be monitored by the change in emission intensity in response to TNT addition [Figure 3A and B]. Upon adding TNT, the emission of the aggregates was gradually quenched. The fluorescence quenching could be clearly observed even at a TNT concentration as low as 0.1 μg/mL, consistent with the previous

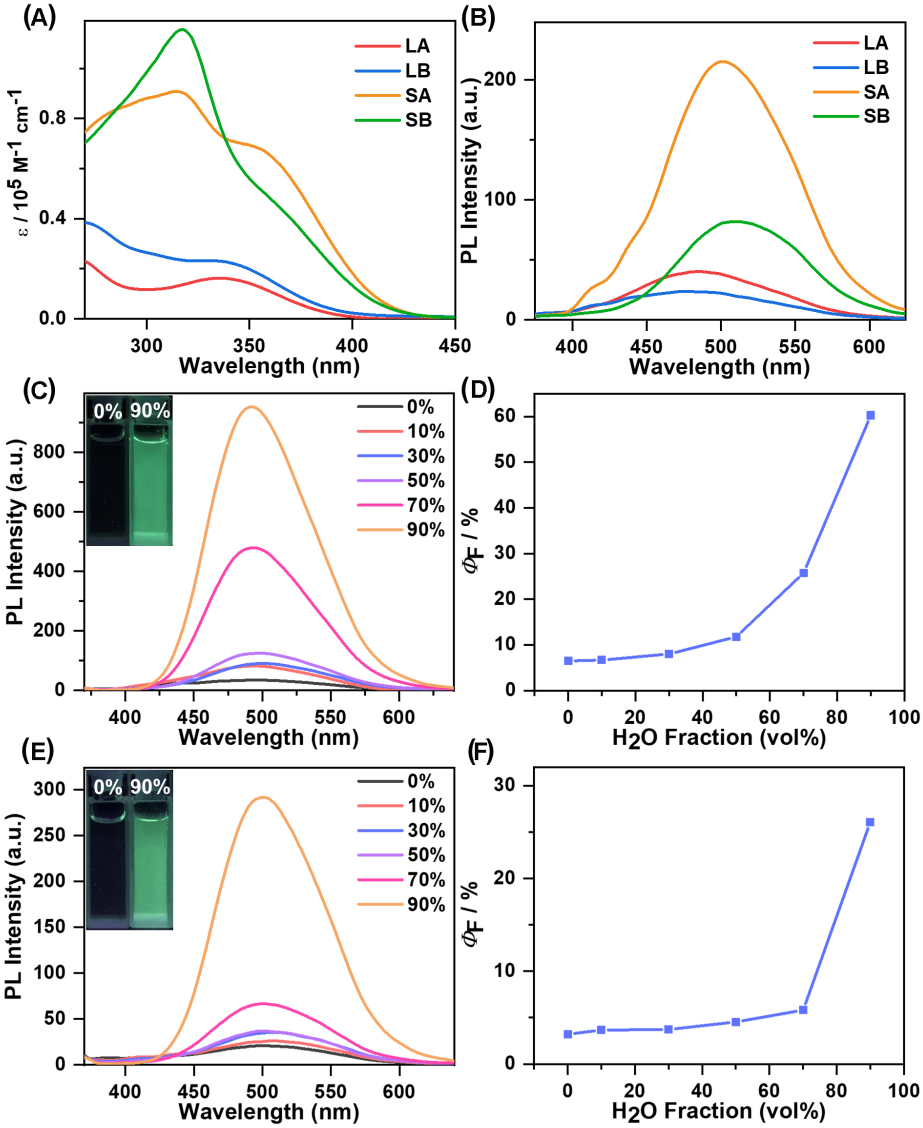

Figure 2. (A) UV-Vis spectra of **LA**, **LB**, **SA**, and **SB** in DMSO (λ_{ex} = 320 nm, c = 10.0 μM). (B) PL spectra of **LA**, **LB**, **SA**, and **SB** in DMSO (λ_{ex} = 320 nm, c = 10.0 μM). PL spectra of **SA** (C) and **SB** (D) recorded in DMSO/H_2O mixtures containing different H_2O fractions. The respective inserts show **SA** and **SB** dissolved in DMSO/H_2O with 0% (left) and 90% H_2O (right). Quantum yields of **SA** (E) and **SB** (F) versus increasing H_2O fractions in DMSO/H_2O mixtures, determined using rhodamine B (Φ_F = 69.0%) at 365 nm (λ_{ex} = 320 nm, c = 1.00 μM).

report[12]. Impressively, although metallacycles **SA** and **SB** had the same components, their quenching efficiency and quenching rate by TNT were completely different. For metallacycle **SB**, quenching efficiency was 21.41% when 0.1 μg/mL of TNT was added to its solution, while it was only 8.86% for **SA** under the same condition. For 10.0 μg/mL TNT concentration, the initial fluorescence intensity of **SB** reduced by 96.76%, but only 76.79% for **SA**. The fluorescence quenching of **SA** could reach 97.68% only when the TNT concentration was increased to 100 μg/mL [Figure 3C]. To determine the quenching constants of metallacycles **SA** and **SB** with TNT, the respective relative fluorescence intensity (I_0/I) was plotted against the TNT concentration. Upon applying a linear Stern-Volmer equation $I_0/I = K[TNT] + 1$[2], from the mean of linear fitting, the quenching constants of **SB** were calculated to be 7.289×10^5 M^{-1}. However, the best fit

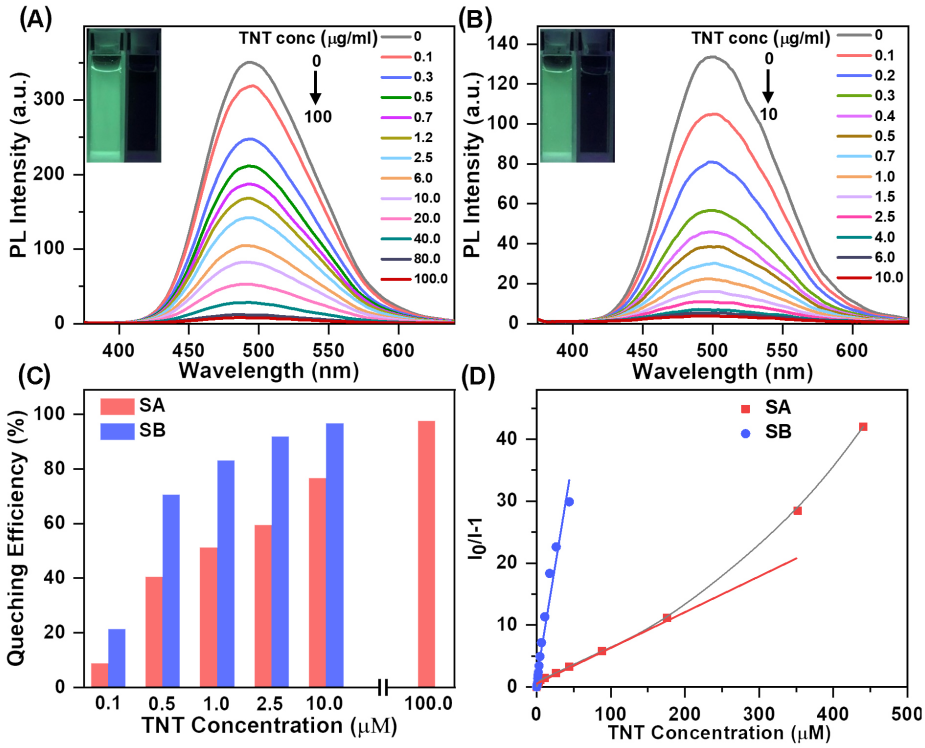

Figure 3. Fluorescence emission spectra of metallacycles **SA** (A) and **SB** (B) in a DMSO/H_2O (1/9) mixture containing different amounts of TNT (λ_{ex} = 320 nm, c = 1.00 μM). (C) The fluorescence quenching efficiencies of metallacycles **SA** and **SB** at different TNT concentrations in a DMSO/H_2O (1:9) mixture. (D) Plot of relative fluorescence intensities (I_0/I, I = peak intensity and I_0 = peak intensity at [TNT] = 0 μM) versus TNT concentrations in a DMSO/H_2O (1:9) mixture (λ_{ex} = 320 nm, c = 1.00 μM).

was obtained with the linear fitting for metallacycle **SA** when the TNT concentration was lower than 176 μg/mL, and the quenching constant was calculated to be 5.774×10^4 M^{-1}. With the further increase of TNT concentration, the quenching process of **SA** showed a curvy enhancement [Figure 3D]. The structural differences of metallacycles **SA** and **SB** led to the large difference in their quenching constants. The key mechanism in binding TNT with chromophoric receptors was generally considered to be through the π-π stacking interactions. Since **SA** is a rhombic metallacycle with a curved structure, its π-π stacking interactions with TNT was hindered, which further affected the fluorescence quenching effect.

CONCLUSION

Two TPE-based metallacycles (named **SA** and **SB**) were constructed using cis-trans isomers of a TPE-based dipyridyl ligand and 120° di-Pt(II) acceptor. The rhombus metallacycle **SA** constructed with the trans-TPE-based dipyridyl ligand had a more curved structure than the rhombus metallacycle **SB** constructed with the cis-TPE-based dipyridyl ligand. The curved **SA** structure restricted the molecular motions of the aryl groups on TPE, resulting in the CIE phenomenon and remarkable light-emitting properties. In addition, **SA** with twisted configuration and high quantum yield showed better fluorescence stability than **SB** in the presence of TNT. This work provides a new platform to explore the relationship between the conformation of the AIE group and the corresponding photophysical properties.

DECLARATIONS

Acknowledgments

This study was supported by the National Natural Science Foundation of China (22071079 for Wang M). The authors thank the staff from the BL17B beamline of the National Facility for Protein Science in Shanghai (NFPS) at Shanghai Synchrotron Radiation Facility for assistance during data collection.

Authors' contributions

Completed the synthesis, conducted NMR characterization, optical tests, and prepared the draft manuscript: Zeng Y
Performed MS characterization: Li K, Fang F
Performed DFT calculations: Li J, Zhang H
Performed part of the X-ray crystal structure data collection: Yu H
Designed the experiments and wrote the manuscript: Shi J, Hao XQ, Wang M

Availability of data and materials

Not applicable.

Financial support and sponsorship

This study was supported by the National Natural Science Foundation of China (22071079 for Wang M).

Conflicts of interest

All authors declared that there are no conflicts of interest.

Ethical approval and consent to participate

Not applicable.

Consent for publication

Not applicable.

REFERENCES

1. Leung CW, Hong Y, Chen S, Zhao E, Lam JW, Tang BZ. A photostable AIE luminogen for specific mitochondrial imaging and tracking. *J Am Chem Soc* 2013;135:62-5. DOI PubMed
2. Liu J, Zhong Y, Lu P, et al. A superamplification effect in the detection of explosives by a fluorescent hyperbranched poly(silylenephenylene) with aggregation-enhanced emission characteristics. *Polym Chem* 2010;1:426-9. DOI
3. Yang SK, Shi X, Park S, Ha T, Zimmerman SC. A dendritic single-molecule fluorescent probe that is monovalent, photostable and minimally blinking. *Nat Chem* 2013;5:692-7. DOI PubMed PMC
4. Zhang Z, Guo K, Li Y, et al. A colour-tunable, weavable fibre-shaped polymer light-emitting electrochemical cell. *Nature Photon* 2015;9:233-8. DOI
5. Hoeben FJ, Jonkheijm P, Meijer EW, Schenning AP. About supramolecular assemblies of pi-conjugated systems. *Chem Rev* 2005;105:1491-546. DOI PubMed
6. Luo J, Xie Z, Lam JW, et al. Aggregation-induced emission of 1-methyl-1,2,3,4,5-pentaphenylsilole. *Chem Commun (Camb)* 2001:1740-1. DOI PubMed
7. Mei J, Leung NL, Kwok RT, Lam JW, Tang BZ. Aggregation-induced emission: together we shine, united we soar! *Chem Rev* 2015;115:11718-940. DOI PubMed
8. Qin Y, Wang Y, Yang H, Zhu W. Recent advances on the construction of diarylethene-based supramolecular metallacycles and metallacages via coordination-driven self-assembly. *CS* 2021. DOI
9. Newkome GR, Moorefield CN. From 1 → 3 dendritic designs to fractal supramacromolecular constructs: understanding the pathway to the Sierpiński gasket. *Chem Soc Rev* 2015;44:3954-67. DOI PubMed
10. Yan X, Wang H, Hauke CE, et al. A suite of tetraphenylethylene-based discrete organoplatinum(ii) metallacycles: controllable

structure and stoichiometry, aggregation-induced emission, and nitroaromatics sensing. *J Am Chem Soc* 2015;137:15276-86. DOI PubMed

11. Guo Z, Li G, Wang H, et al. Drum-like metallacages with size-dependent fluorescence: exploring the photophysics of tetraphenylethylene under locked conformations. *J Am Chem Soc* 2021;143:9215-21. DOI PubMed
12. Qin A, Lam JWY, Tang L, et al. Polytriazoles with aggregation-induced emission characteristics: synthesis by click polymerization and application as explosive chemosensors. *Macromolecules* 2009;42:1421-4. DOI

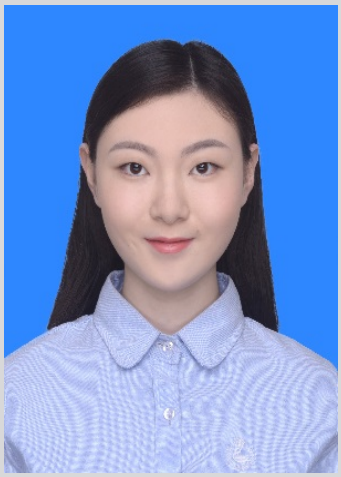

Yunting Zeng

Yunting Zeng obtained her BS from Jilin University, China in 2018. In the same year, she started her PhD study under the guidance of Professor Ming Wang from Jilin University (China). She focuses on the construction of 2D and 3D luminescent supramolecular architectures.

Junjuan Shi

Junjuan Shi received her BS in 2016 from Changchun University of Technology. After that, she obtained her PhD degree under the guidance of Professor Ming Wang at Jilin University (China) in 2021. She joined the group of Prof. Xiaopeng Li at the University of South Florida (US) as a joint training of doctoral student during 2018–2020. Currently, she is a Postdoctoral Researcher at Jilin University under the "Dingxin Scholar Program." Her research interests include the construction and function of 2D supramolecular architectures.

Kehuan Li

Kehuan Li received his BS from Jilin University, China in 2018. After that, he started PhD study under the guidance of Professor Ming Wang from Jilin University (China). He joined the group of Prof. Xiaopeng Li at the Shenzhen University (China) as a joint training of doctoral student during 2021–2022. His research interests include the self-assembly and self-sorting behavior based on dissymmetrical ligands.

Jiaqi Li

Jiaqi Li received her BS from Shanxi Datong University in 2017. Now she is a PhD student under the supervision of Professor Houyu Zhang in the College of Chemistry, Jilin University. Her research is focused on the molecular design of highly efficient organic light emitting materials using first-principles computational methods.

Hao Yu

Hao Yu received his BS in 2017 from Changchun University of Technology. In the same year, he started his PhD study under the guidance of Professor Ming Wang from Jilin University (China). He focuses on the construction and function of 3D supramolecular architectures, self-assembly based on dissymmetrical ligands.

Fang Fang

Fang Fang received her PhD in chemistry from the Cleveland State University and Cleveland Clinic Foundation (USA) in 2012 under the supervision of Prof. Qing Wang. She obtained a PharmD in Pharmacy from University of South Florida (USA) in 2018. She now works as a senior technician at Instrumental Analysis Center of Shenzhen University. Her research interests focus on characterization of synthetic macromolecules and nanomaterials.

Xin-Qi Hao

Xin-Qi Hao received his BSc and PhD degrees in 2002 and 2007, respectively, supervised by Prof. Mao-Ping Song from the College of Chemistry, Zhengzhou University. In 2012, he joined Professor Michael J. Krische's group in University of Texas at Austin (USA) as a Postdoctoral Researcher. In 2007, he joined the college of Chemistry, Zhengzhou University and became a full professor in 2016. His research interests focus on organometallic chemistry, organic synthetic chemistry, and supramolecular chemistry.

Houyu Zhang

Houyu Zhang earned his PhD degree in the department of chemistry at Hong Kong University of Science and Technology in 2002. During 2002-2005, he was a postdoctoral researcher in the department of physics, University of Modena and Reggio Emilia, Italy. After that, he became an associate professor at the Jilin University in 2005. Now he is a professor in the college of chemistry, Jilin University. His research is directed at understanding of supramolecular aggregates and organic photoelectronic materials with the emphasis on structure-property relationships, charge transport properties, and excited state dynamics.

Ming Wang

Ming Wang received his PhD from the Changchun Institute of Applied Chemistry, Chinese Academy of Sciences in 2010. Then he joined Professor Pooi See Lee's group in Nanyang Technological University (Singapore) as a Postdoctoral Researcher. In 2013, he continued as a postdoctoral researcher in Xiaopeng Li's group in Texas State University (USA). He is now a professor in the College of Chemistry of Jilin University. His research interests focus on the construction of metallo-supramolecular architectures, self-assembly based on dissymmetrical ligands, and function development of discrete supramolecular structures.